

# The $\sigma$ and $\rho$ coupling constants for the charmed and beauty mesons

Hee-Jin Kim<sup>1,\*</sup> and Hyun-Chul Kim<sup>1,2,†</sup>

<sup>1</sup>*Department of Physics, Inha University, Incheon 22212, Korea*

<sup>2</sup>*School of Physics, Korea Institute for Advanced Study (KIAS), Seoul 02455, Republic of Korea*

(Dated: June, 2020)

We investigate the  $\sigma$  and  $\rho$  coupling constants for the  $DD$  and  $D^*D^*$  interactions, based on correlated  $2\pi$  exchange in the  $DD$  and  $D^*D^*$  interactions. Starting from the  $D\bar{D} \rightarrow \pi\pi$  and  $D^*\bar{D}^* \rightarrow \pi\pi$  amplitudes derived in the pseudophysical region ( $4m_\pi^2 \leq t \leq 52m_\pi^2$ ) with the  $S$ - and  $P$ -wave  $2\pi$  correlations considered, we obtain the spectral functions for the  $DD \rightarrow DD$  and  $D^*D^* \rightarrow D^*D^*$  amplitude with correlated  $S$ - and  $P$ -wave  $2\pi$  exchanges. Using the pole approximation, we estimate the  $DD\sigma$ ,  $DD\rho$ ,  $D^*D^*\sigma$ , and  $D^*D^*\rho$  coupling constants. We extended phenomenologically the present results to the region in  $t \leq 0$  and compare them with those from lattice QCD. The results are also compared with those of other models. We also present the results of the  $BB\sigma$ ,  $BB\rho$ ,  $B^*B^*\sigma$ , and  $B^*B^*\rho$  coupling constants. We observe that it is unlikely that the  $\sigma$  and  $\rho$  coupling constants for the  $B$  and  $B^*$  mesons are the same as those for the  $D$  and  $D^*$  mesons. On the contrary, they are quite larger than those for the charmed mesons.

Keywords:  $\sigma$  and  $\rho$  coupling constants for heavy mesons,  $H\bar{H} \rightarrow \pi\pi$  and  $H^*\bar{H}^* \rightarrow \pi\pi$  pseudophysical amplitudes, correlated  $2\pi$  exchange in the  $DD$  and  $D^*D^*$  interactions

arXiv:1912.11622v6 [hep-ph] 18 Jun 2020

---

\* heejin.kim@inha.edu

† hchkim@inha.ac.kr

## I. INTRODUCTION

Understanding exotic heavy mesons has been one of the most important issues in hadronic physics (see, for example, recent reviews [1–5]). In 2003, a charmonium-like state  $X(3872)$  was newly found by the Belle Collaboration [6] and was subsequently confirmed by other experiments [7–10]. The mass of the  $X(3872)$  turns out to be approximately few tens of MeV lower than the  $P$ -wave charmonium  $\chi_{c1}(2P)$  predicted by the heavy-quark potential models [11–16]. The Belle Collaboration [6] also measured the upper limit on the ratio of the partial decay widths  $\Gamma(X(3872) \rightarrow \gamma\chi_{c1})/\Gamma(X(3872) \rightarrow \pi^+\pi^-J/\psi) < 0.89$ , which was very different from the predictions of Ref. [17] in which the decays of  $D$ -wave missing charmoniums were considered. Though there was an argument that the  $X(3872)$  is still a  $1^3D_2$  charmonium state [18], these discrepancies led to various theoretical interpretations on the  $X(3872)$ . It can be regarded as a tetraquark state [19–21] or as a hybrid exotic state [22]. It is also plausible to consider it as a molecular state of  $D$  and  $\bar{D}^*$  mesons [23–27], since its mass is very close to the sum of the masses of the  $D$  and  $D^*$  mesons ( $M_{X(3872)} - M_{D^{*0}} - M_{D^0} = 0.01 \pm 0.18$  MeV), which resembles the deuteron consisting of the proton and the neutron. The quantum number of the  $X(3872)$  is now established as an isosinglet state with  $J^{PC} = 1^{++}$  [28].

In addition to the  $X(3872)$  meson, a number of new heavy mesons has been experimentally observed over the last decade (see, for example, glossary of exotic states summarized in Appendix of Ref. [3]). Many of them can be regarded as molecular states. While the pion exchange is a main ingredient for the description of those exotic mesons as molecular states, the  $\sigma$  meson exchange may come into play, since it provides a strong attraction in medium range of the interaction so as to make two heavy mesons such as  $D$  ( $D^*$ ) and  $\bar{D}^*$  ( $D^*$ ) bound. However, the coupling constants for the  $DD\sigma$  and  $D^*D^*\sigma$  vertices are not well known both theoretically and experimentally, so that these couplings have been estimated by using either the nonlinear sigma model or quark models [29–32]. Moreover, the  $D^*D^*\sigma$  coupling constant was taken to be the same as the  $DD\sigma$  one in many theoretical works with the heavy-quark spin symmetry assumed. On the other hand, the  $\sigma$  exchange in the  $NN$  interaction is known to be a parametrization of the correlated  $2\pi$  exchange, based on the pole approximation [33–35], which approximates the broad mass distribution of the  $\sigma$  meson to a sharp mass. This  $\sigma$ -exchange contribution has been an essential part of providing the strong attraction in the intermediate range of the  $NN$  potential. In fact, the  $S$ -wave correlated  $2\pi$  exchange has been employed in predicting the  $DD$  and  $BB$  bound states [36] already. Since one  $\pi$  exchange is not allowed between the pseudoscalar heavy mesons,  $\sigma$  exchange plays a crucial role in examining the bound states of the  $DD$  and  $BB$  system. Similarly,  $\rho$ -meson exchange can be also regarded as a parametrization of the correlated  $2\pi$  exchange in the  $P$ -wave (vector-isovector) channel [34, 35].

In the present work, we derive the five different coupling constants:  $g_{DD\sigma}$ ,  $g_{DD\rho}$ ,  $g_{D^*D^*\sigma}$ ,  $g_{D^*D^*\rho}$ , and  $f_{D^*D^*\rho}$ , based on the pseudophysical  $D\bar{D} \rightarrow \pi\pi$  and  $D^*\bar{D}^* \rightarrow \pi\pi$  amplitudes. The  $NN\sigma$  coupling constant can be determined by using the pseudophysical  $N\bar{N} \rightarrow \pi\pi$  amplitudes in the  $NN$  interaction. In Ref. [37], the  $N\bar{N} \rightarrow \pi\pi$  amplitudes in the pseudophysical region with  $\pi\pi$  rescattering was constructed, from which the  $NN\sigma$  coupling constant with broad width can be extracted. In this work, we closely follow the theoretical technique developed in Ref. [37]. In fact, the same method was adopted in the full Bonn potential for the  $NN$  interaction,  $\sigma'$  exchange being replaced by the *correlated*  $2\pi$  exchange developed in this way [35]. Later, this approach was also employed in the Jülich-Bonn potential for the hyperon-nucleon interaction [38]. Thus, we will take this well-established method to determine the  $\sigma$  coupling constants for the  $D$  and  $D^*$ . We will also apply this to the  $\sigma$  coupling constants for the  $B$  and  $B^*$  mesons.

The schematic diagram for the correlated  $2\pi$  exchange in the  $DD$  and  $D^*D^*$  interactions is drawn in Fig. 1. To

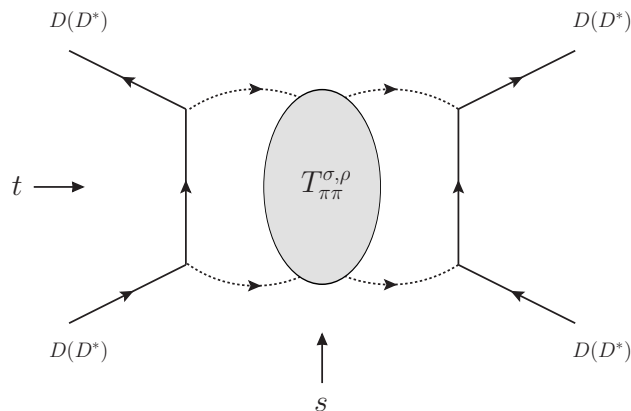


FIG. 1. Schematic diagram for the correlated  $2\pi$  exchange.

determine these coupling constants, we first formulate the off-shell  $D\bar{D} \rightarrow \pi\pi$  and  $D^*\bar{D}^* \rightarrow \pi\pi$  amplitudes in the pseudophysical region ( $4m_\pi^2 \leq t \leq 52m_\pi^2$ ), where  $t$  is the total energy squared in the center of momentum (CM) system, using the effective Lagrangians. We want to mention that there is one caveat. The kaon and antikaon ( $K\bar{K}$ ) channel is open at around  $50m_\pi^2$ . Thus, it is natural to include the  $K\bar{K}$  channel in a coupled-channel formalism. However, since there is no information on the relevant coupling constants, it is inevitable to introduce additional uncertainties in the present calculation by including the  $K\bar{K}$  channel. Thus, we will consider only the  $\pi\pi$  channel. Then, we combine the  $D\bar{D} \rightarrow \pi\pi$  amplitudes with the off-shell  $\pi\pi$  amplitudes evaluated within the Jülich  $\pi\pi$  model [39, 40] but modified in a covariant way. The model described very well the phase shifts of  $\pi\pi$  scattering in both the scalar-isoscalar and vector-isovector channels. The  $\pi\pi$  amplitudes with meson-exchange picture is the most consistent and convenient one for the present approach, because we will construct the off-shell Born amplitudes for the  $D\bar{D} \rightarrow \pi\pi$  and  $D^*\bar{D}^* \rightarrow \pi\pi$  based on the effective Lagrangians. We want to mention that the method we adopt in this work is basically the same as shown in Ref. [35, 37]. The two-body unitarity allows one to construct the spectral functions for the  $D\bar{D}$  and  $D^*\bar{D}^*$  amplitudes. Having derived these spectral functions, one can directly compute the coupling constants listed above by using the dispersion relation. For completeness, we also present the results of the  $\sigma$  and  $\rho$  coupling constants for the  $B$  and  $B^*$  mesons.

The present work is organized as follows: In Section II, we show how to derive the spectral functions from which the coupling constants can be determined. In Section III, we discuss the present results in comparison with those of other works. The last Section is devoted to summary and conclusion.

## II. GENERAL FORMALISM

### A. $D\bar{D} \rightarrow \pi\pi$ and $D^*\bar{D}^* \rightarrow \pi\pi$ amplitudes

We start with the effective Lagrangian from HQET [41–44]

$$\mathcal{L} = ig\text{tr} [H_b A_{ba} \gamma_5 \bar{H}_a], \quad (1)$$

where the heavy meson field  $H_b$  is given as

$$H_b = \frac{1 + \not{v}}{2} [P_b^{*\mu} \gamma_\mu - P_b \gamma_5], \quad (2)$$

and the axial-vector field  $A_{ba}^\mu$  is expressed as

$$A_{ba}^\mu = \frac{1}{2}(\xi^\dagger \partial^\mu \xi - \xi \partial^\mu \xi^\dagger) = \frac{i}{f_\pi} \partial^\mu \mathcal{M}_{ba} + \dots \quad (3)$$

with the pseudoscalar meson field  $\mathcal{M}$

$$\mathcal{M} = \begin{pmatrix} \frac{\pi^0}{\sqrt{2}} + \frac{\eta}{\sqrt{6}} & \pi^+ & K^+ \\ \pi^- & -\frac{\pi^0}{\sqrt{2}} + \frac{\eta}{\sqrt{6}} & K^0 \\ K^- & \bar{K}^0 & -\frac{2\eta}{\sqrt{6}} \end{pmatrix}. \quad (4)$$

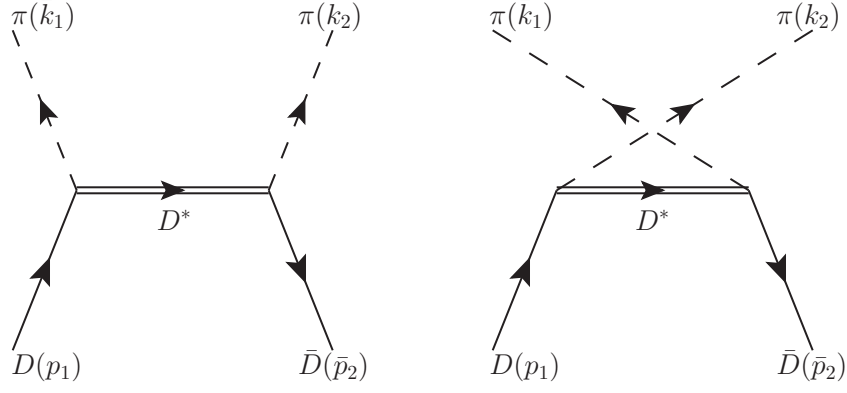
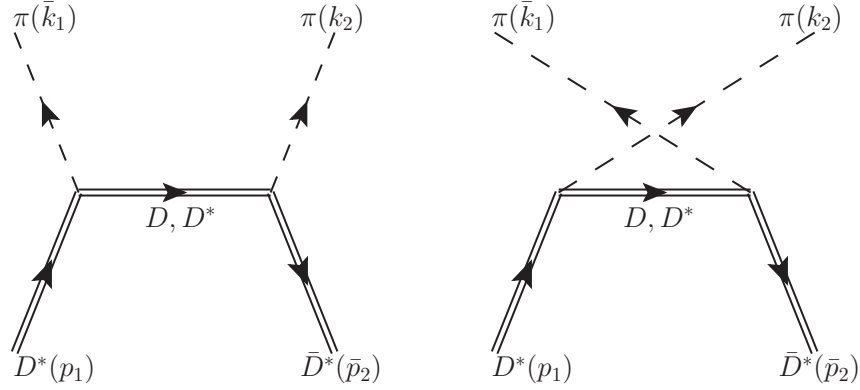
The pseudo-Nambu-Goldstone (pNG) field or the coset field  $\xi(x)$  [45], which realizes the emergence of the pNG field due to the spontaneous breakdown of chiral symmetry, is defined as

$$\xi(x) = \exp[i\mathcal{M}(x)/f_\pi] \quad (5)$$

with the pion decay constant  $f_\pi = 132$  MeV normalized. Since we need only the single pNG field, we keep the expansion to linear order with respect to  $\mathcal{M}$ . The Dirac conjugate of the heavy meson field  $\bar{H}_a$  is written as  $\bar{H}_a = \gamma_0 H^\dagger \gamma_0$ . The effective Lagrangians for  $PP^*M$  and  $P^*P^*M$  couplings are then

$$\begin{aligned} \mathcal{L}_{PP^*M} &= -\frac{2g}{f_\pi} P^{*\mu} \partial_\mu \mathcal{M}_{ba} P^\dagger + \text{h.c.}, \\ \mathcal{L}_{P^*P^*M} &= \frac{2gi}{f_\pi} P_b^{*\beta} \partial^\mu \mathcal{M}_{ba} P_a^{*\alpha\dagger} \varepsilon_{\alpha\beta\mu\nu} v^\nu, \end{aligned} \quad (6)$$

where  $f_\pi$  denotes the pion decay constant of which the value is taken from the experimental one,  $f_\pi = 132$  MeV. Note that the parity conservation does not allow the  $DD\pi$  vertex.

FIG. 2. Feynman diagrams for  $D\bar{D} \rightarrow \pi\pi$ FIG. 3. Feynman diagrams for  $D^*\bar{D}^* \rightarrow \pi\pi$ 

Using Eqs. (6), we can compute the off-shell Born amplitudes for the  $D\bar{D} \rightarrow \pi\pi$  and  $D^*\bar{D}^* \rightarrow \pi\pi$  processes. The corresponding Feynman diagrams are given in Fig. 2. As for the  $D\bar{D} \rightarrow \pi\pi$  process, we need to consider only  $D^*$ -meson exchange, whereas we have to consider both  $D$ - and  $D^*$ -meson exchanges for the  $D^*\bar{D}^* \rightarrow \pi\pi$  process. As depicted in Figs. 2 and 3,  $p_1$  and  $\bar{p}_2$  stand for four-momenta for the initial  $D$  ( $D^*$ ) and  $\bar{D}$  ( $\bar{D}^*$ ) mesons, and  $\bar{k}_1$  and  $k_2$  denote those for the final pions, respectively. In the CM frame, they are expressed as

$$\begin{aligned} p_1 &= (E_p, \mathbf{p}), & \bar{p}_2 &= (E_p, -\mathbf{p}), \\ \bar{k}_1 &= (\omega_k, \mathbf{k}), & k_2 &= (\omega_k, -\mathbf{k}), \end{aligned} \quad (7)$$

where

$$E_p = \sqrt{M_{D(D^*)}^2 + \mathbf{p}^2}, \quad \omega_k = \sqrt{m_\pi^2 + \mathbf{k}^2}. \quad (8)$$

The conservation of the total momentum is given as

$$p_1 + \bar{p}_2 = \bar{k}_1 + k_2. \quad (9)$$

The Mandelstam variables in the  $t$  channel are defined as

$$\begin{aligned} s &= (p_1 - \bar{k}_1)^2 = (\bar{p}_2 - k_2)^2 = p_1^2 + \bar{k}_1^2 - 2p_1 \cdot \bar{k}_1, \\ t &= (p_1 + \bar{p}_2)^2 = (\bar{k}_1 + k_2)^2 = p_1^2 + \bar{p}_2^2 + 2p_1 \cdot \bar{p}_2 = \bar{k}_1^2 + k_2^2 + 2\bar{k}_1 \cdot k_2, \\ u &= (p_1 - k_2)^2 = (\bar{p}_2 - \bar{k}_1)^2 = \bar{p}_2^2 + \bar{k}_1^2 - 2\bar{p}_2 \cdot \bar{k}_1, \end{aligned} \quad (10)$$

where  $t$  is just the square of the total energy while  $s$  represents the square of the momentum transfer. Since we are interested in the pseudophysical region and want to combine these Born amplitudes with the  $\pi\pi$  rescattering

amplitude, we have to consider the off-mass shell pion states. Thus, we need to take into account the virtual momenta of the two pions, i.e.,

$$\bar{k}_1^2 = \frac{t}{4} - \mathbf{k}^2, \quad k_2^2 = \frac{t}{4} - \mathbf{k}^2, \quad \bar{k}_1 \cdot k_2 = \frac{t}{4} + \mathbf{k}^2. \quad (11)$$

Since we will use the  $D\bar{D} \rightarrow \pi\pi$  ( $D^*\bar{D}^* \rightarrow \pi\pi$ ) amplitudes to derive the spectral functions of  $D\bar{D} \rightarrow D\bar{D}$  ( $D^*\bar{D}^* \rightarrow D^*\bar{D}^*$ ) with  $2\pi$  unitarity, we need to consider the off-mass shell momenta for pions. The sum of all the Mandelstam variables are expressed in terms of the masses of  $D$  and  $\pi$

$$s + t + u = 2(M_{D(D^*)}^2 + m_\pi^2). \quad (12)$$

with the conservation of the total momentum. Let  $\theta$  be the angle between  $\mathbf{p}$  and  $\mathbf{k}$ . Then,

$$\begin{aligned} s &= M_{D(D^*)}^2 + \frac{t}{4} - \mathbf{k}^2 - 2E_p\omega_k + 2|\mathbf{p}||\mathbf{k}|\cos\theta, \\ t &= 4\omega_k^2 \geq 4m_\pi^2, \\ u &= 2M_{D(D^*)}^2 + 2m_\pi^2 - s - t. \end{aligned} \quad (13)$$

The invariant amplitudes for the  $D\bar{D} \rightarrow \pi\pi$  process are given as

$$\begin{aligned} \mathcal{M}_{\alpha\beta}^s(D\bar{D} \rightarrow \pi\pi) &= g_{DD^*\pi}^2 \frac{\bar{k}_1 \cdot k_2 - \frac{(\bar{k}_1 \cdot q)(k_2 \cdot q)}{M_{D^*}^2}}{s - M_{D^*}^2} \tau_\alpha \tau_\beta, \\ \mathcal{M}_{\alpha\beta}^u(D\bar{D} \rightarrow \pi\pi) &= -g_{DD^*\pi}^2 \frac{\bar{k}_1 \cdot k_2 - \frac{(\bar{k}_1 \cdot q)(k_2 \cdot q)}{M_{D^*}^2}}{u - M_{D^*}^2} \tau_\beta \tau_\alpha. \end{aligned} \quad (14)$$

Similarly, those for the  $D^*\bar{D}^* \rightarrow \pi\pi$  process are obtained as

$$\begin{aligned} \mathcal{M}_{\alpha\beta}^s(D^*\bar{D}^* \rightarrow \pi\pi) &= \left[ g_{DD^*\pi}^2 \frac{(\epsilon^{(\lambda)}(p_1) \cdot \bar{k}_1)(\epsilon^{(\lambda')}(\bar{p}_2) \cdot k_2)}{s - M_D^2} \right. \\ &\quad \left. + 4g_{D^*D^*\pi}^2 \epsilon_{\mu_1\nu_1\rho_1\sigma_1} \epsilon_{\mu_2\nu_2\rho_2\sigma_2} g^{\mu_1\mu_2} \frac{\epsilon^{(\lambda)\nu_1}(p_1) \epsilon^{(\lambda')\nu_2}(\bar{p}_2) p_1^{\sigma_1} \bar{p}_2^{\sigma_2} \bar{k}_1^{\rho_1} k_2^{\rho_2}}{s - M_{D^*}^2} \right] \tau_\alpha \tau_\beta, \\ \mathcal{M}_{\alpha\beta}^u(D^*\bar{D}^* \rightarrow \pi\pi) &= \left[ g_{DD^*\pi}^2 \frac{(\epsilon^{(\lambda)}(p_1) \cdot k_2)(\epsilon^{(\lambda')}(\bar{p}_2) \cdot \bar{k}_1)}{u - M_D^2} \right. \\ &\quad \left. + 4g_{D^*D^*\pi}^2 \epsilon_{\mu_1\nu_1\rho_1\sigma_1} \epsilon_{\mu_2\nu_2\rho_2\sigma_2} g^{\mu_1\mu_2} \frac{\epsilon^{(\lambda)\nu_1}(p_1) \epsilon^{(\lambda')\nu_2}(\bar{p}_2) p_1^{\sigma_1} \bar{p}_2^{\sigma_2} k_2^{\rho_1} \bar{k}_1^{\rho_2}}{u - M_{D^*}^2} \right] \tau_\beta \tau_\alpha. \end{aligned} \quad (15)$$

The total amplitude can be generically expressed in terms of the iso-symmetric amplitude  $\mathcal{M}^{(+)}$  and the iso-antisymmetric amplitude  $\mathcal{M}^{(-)}$

$$\mathcal{M}_{\alpha\beta} = \mathcal{M}^{(+)} \delta_{\alpha\beta} + \mathcal{M}^{(-)} \frac{1}{2} [\tau_\alpha, \tau_\beta], \quad (16)$$

where

$$\mathcal{M}^{(+)} = \mathcal{M}^s + \mathcal{M}^u, \quad \mathcal{M}^{(-)} = \mathcal{M}^s - \mathcal{M}^u. \quad (17)$$

Note that the isospin amplitudes for  $J = 0$  and  $J = 1$  are respectively related to  $\mathcal{M}^{(+)}$  and  $\mathcal{M}^{(-)}$  as in the case of the  $N\bar{N} \rightarrow \pi\pi$  amplitudes [35, 46]

$$\mathcal{M}^{(+)} = -\frac{1}{\sqrt{6}} \mathcal{M}_{T=0}, \quad \mathcal{M}^{(-)} = -\frac{1}{2} \mathcal{M}_{T=1}. \quad (18)$$

In order to compute the amplitudes given in Eqs. (14) and (15), we have to introduce the form factors at each vertex. We employ a Gaussian-type form factor defined as

$$F(s) = \exp \left[ \frac{s - M_{\text{ex}}^2}{\Lambda_{\text{ex}}^2} \right], \quad (19)$$

where  $M_{\text{ex}}$  represents either the mass of  $D$  meson or that of the  $D^*$  meson.  $\Lambda_{\text{ex}}$  denotes the cutoff mass corresponding to the exchange particle. In Ref. [35], the value of the cutoff mass  $\Lambda_N$  ( $\Lambda_\Delta$ ) was taken to be around 1.5 GeV (1.7 GeV) when the spectral functions for the  $NN\sigma$  and  $NN\rho$  coupling constants were investigated. However, the masses of the  $D$  and  $D^*$  mesons are approximately two times larger than the nucleon or the  $\Delta$  isobar, the values of the cutoff mass for the  $DD\pi$  and  $D^*D^*\pi$  vertices should be taken to be larger than those for the  $NN\pi$  and  $N\Delta\pi$  ones. Otherwise, the amplitudes depend too sensitively on the cutoff masses, because their numerical values are too close to the masses of the exchanged  $D$  or  $D^*$  mesons. Moreover, a recent work on the electromagnetic form factors of the heavy baryons [47] has shown that the heavy baryon is a much more compact object in comparison with the proton. It indicates that the cutoff mass of the parametrized heavy-baryon electric form factor should be larger than that of the proton at least by about a factor 1.6, because the cutoff mass is implicitly related to the corresponding particle. Thus, we will use the values of the cutoff masses  $\Lambda_D = 2.5$  GeV and  $\Lambda_{D^*} = 2.8$  GeV in the present work. Moreover, if one uses smaller values of the cutoff masses, one can not get stable results for the form factors corresponding to the coupling constants in the physical  $t$  region ( $t \leq 0$ ). At a certain value of  $-t$ , the  $\sigma$  coupling constant even vanishes, which leads to unphysical results.

As far as an explicit form of the form factors is concerned, one could utilize the well-known monopole- or dipole-type form factor. However, we find that such types of the form factors do not suppress enough the Born amplitudes as the total energy increases. For example, the Born amplitudes for the  $D^*\bar{D}^* \rightarrow \pi\pi$  process given in Eq. (15) has a strong dependence on  $t$ . In particular, the second terms in the  $s$ - and  $u$ -channel amplitudes contain the four momenta in the numerator, which make the amplitudes too large as  $t$  increases. To tame this behavior, we employ the Gaussian-type form factor at each vertex.

### B. Rescattering equation and spectral functions

Once the off-shell Born amplitudes have been evaluated, the next step is to compute the rescattering equation that combines the off-shell  $D\bar{D} \rightarrow \pi\pi$  and  $D^*\bar{D}^* \rightarrow \pi\pi$  amplitudes with the off-shell  $\pi\pi$  amplitudes. As shown in Fig. 4,

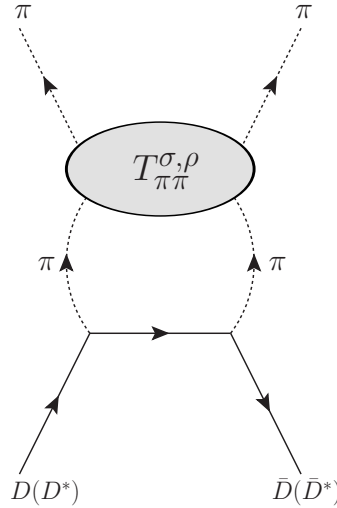


FIG. 4. Rescattering equation

we need to incorporate the  $\pi\pi$  interaction in the course of the  $D\bar{D} \rightarrow \pi\pi$  and  $D^*\bar{D}^* \rightarrow \pi\pi$  processes. This can be achieved by considering the Blankenbecler-Sugar (BbS) equation [37, 48], which was derived by the three-dimensional reduction of the Bethe-Salpeter equation:

$$\mathcal{M}_{D\bar{D}(D^*\bar{D}^*) \rightarrow \pi\pi}(p, p'; t) = \mathcal{M}_{D\bar{D}(D^*\bar{D}^*) \rightarrow \pi\pi}^{\text{Born}}(p, p'; t) + \frac{1}{(2\pi)^3} \int d^3q \frac{1}{\omega_q} \frac{\mathcal{M}_{D\bar{D}(D^*\bar{D}^*) \rightarrow \pi\pi}(p, q; t) \tau(q, p'; t)}{t - 4\omega_q^2 + i\epsilon}. \quad (20)$$

Since we consider only the scalar-isoscalar ( $J = 0, T = 0$ ) and vector-isovector channels ( $J = 1, T = 1$ ), which will provide the  $DD(D^*D^*)\sigma$ - and  $DD(D^*D^*)\rho$ -meson coupling constants respectively, we can make a partial-wave expansion of the amplitudes so that we get the partial-wave rescattering equation for the partial-wave amplitudes

with  $J$  and  $T$  given:

$$\mathcal{M}_{JT}^{D\bar{D}(D^*\bar{D}^*)\rightarrow\pi\pi}(t) = \mathcal{M}_{JT}^{D\bar{D}(D^*\bar{D}^*)\rightarrow\pi\pi,\text{Born}}(t) + \frac{1}{2\pi^2} \int dq q^2 \frac{\mathcal{M}_{JT}^{D\bar{D}(D^*\bar{D}^*)\rightarrow\pi\pi}(p, q; t) \tau_{JT}^{\pi\pi}(q, p'; t)}{2\omega_q(t - 4\omega_q^2 + i\varepsilon)}, \quad (21)$$

where  $\tau_{JT}^{\pi\pi}$  denote the off-shell  $\pi\pi$  amplitudes, which were taken from the Jülich  $\pi\pi$  scattering model [39, 40]<sup>1</sup>.

Next, we consider the unitarity of the  $S$ -matrix, i.e.,

$$SS^\dagger = S^\dagger S = 1. \quad (22)$$

Since the  $S$ -matrix for two-body processes is expressed in terms of the  $\mathcal{M}$ -matrix or the Feynman invariant amplitude

$$S_{fi} = \delta_{fi} + i(2\pi)^4 \delta(p_3 + p_4 - p_1 - p_2) \mathcal{M}_{fi}, \quad (23)$$

we can get the unitary relation

$$S_{fn} S_{ni}^\dagger = \delta_{fi} + i(2\pi)^4 \delta^{(4)}(P_f - P_i) (\mathcal{M}_{fi} - \mathcal{M}_{fi}^\dagger) + (2\pi)^8 \delta^{(4)}(P_f - P_i) \sum_n \mathcal{M}_{fn} \mathcal{M}_{ni}^\dagger \delta^{(4)}(P_f - P_n) = \delta_{fi}, \quad (24)$$

which leads to the following relation

$$2\text{Im}\mathcal{M}_{fi} = (2\pi)^4 \sum_n \delta^{(4)}(P_f - P_n) \mathcal{M}_{fn} \mathcal{M}_{ni}^\dagger, \quad (25)$$

where the summation runs over the  $2\pi$  states, which is often called two-body unitarity. More explicitly, we can write it as

$$2\text{Im}\mathcal{M}_{D\bar{D}(D^*\bar{D}^*)} = (2\pi)^4 \sum_n \delta^{(4)}(P_f - P_n) \mathcal{M}_{D\bar{D}(D^*\bar{D}^*)\rightarrow\pi\pi} \mathcal{M}_{\pi\pi\rightarrow D\bar{D}(D^*\bar{D}^*)}^\dagger. \quad (26)$$

Since we consider the two-body intermediate states, the unitarity relation can be explicitly written as

$$2\text{Im}\mathcal{M}_{D\bar{D}(D^*\bar{D}^*)} = (2\pi)^4 \frac{1}{2!} \int \frac{d^3q_1}{(2\pi)^3 2\omega_1} \frac{d^3q_2}{(2\pi)^3 2\omega_2} \delta^{(4)}(p_1 + p_2 - q_1 - q_2) \mathcal{M}_{D\bar{D}(D^*\bar{D}^*)\rightarrow\pi\pi} \mathcal{M}_{\pi\pi\rightarrow D\bar{D}(D^*\bar{D}^*)}^\dagger. \quad (27)$$

Note that  $1/2!$  is introduced because of the Bose symmetry. Having carried out the integrals, we obtain

$$\text{Im}\mathcal{M}_{D\bar{D}(D^*\bar{D}^*)} = \frac{1}{128\pi^2} \sqrt{\frac{t - 4m_\pi^2}{t}} \int d\Omega |\mathcal{M}_{D\bar{D}(D^*\bar{D}^*)\rightarrow\pi\pi}|^2. \quad (28)$$

Taking into account the isospin factors, we find the following relation

$$\mathcal{M}_{D\bar{D}(D^*\bar{D}^*)} = 3\mathcal{M}_{D\bar{D}(D^*\bar{D}^*)}^{(+)} + 2\mathcal{M}_{D\bar{D}(D^*\bar{D}^*)}^{(-)} \boldsymbol{\tau}_1 \cdot \boldsymbol{\tau}_2. \quad (29)$$

In fact, we need to make a partial-wave expansion in the unitarity relation, since we want to extract the scalar-isoscalar ( $\sigma$ ) and vector-isovector ( $\rho$ ) channels from the  $D\bar{D} \rightarrow D\bar{D}$  and  $D\bar{D} \rightarrow \pi\pi$  amplitudes. Since the particles involved are all pseudoscalar particles, we can expand the amplitudes as

$$\mathcal{M}_{D\bar{D}} = \sum_J (2J+1) P_J(\cos\theta) M_J(t, \cos\theta), \quad \mathcal{M}_{D\bar{D}\rightarrow\pi\pi} = \sum_J (2J+1) P_J(\cos\theta) A_J(t, \cos\theta). \quad (30)$$

Thus, we obtain the spectral functions for the  $D\bar{D}$  amplitude

$$\rho_{JT}^{(\pm)}(t) = \text{Im}M_{JT}^{D\bar{D}} = \frac{1}{32\pi} \sqrt{\frac{t - 4m_\pi^2}{t}} |A_{JT}^{D\bar{D}\rightarrow\pi\pi}|^2. \quad (31)$$

---

<sup>1</sup> One could argue that a modern  $\pi\pi$  amplitude would serve better for the present work. While the modern  $\pi\pi$  amplitudes developed in chiral perturbation theory with the Roy-like equations are certainly theoretically more rigorous, the present  $\pi\pi$  amplitudes taken from the meson-exchange picture are consistent and well fitted in the present approach and furthermore provide the full off-mass-shellness that is essential in solving the rescattering equations.

Note that we have to subtract the Born amplitudes from Eq. (31), i.e., the spectral function is in fact defined as

$$\rho_{00}^{(+)}(t) = \text{Im}M_{00}^{D\bar{D}} - \text{Im}M_{00}^{D\bar{D},\text{Born}}, \quad \rho_{11}^{(-)}(t) = \text{Im}M_{11}^{D\bar{D}} - \text{Im}M_{11}^{D\bar{D},\text{Born}}. \quad (32)$$

Using the dispersion relation, we find the  $DD$  amplitude with correlated  $2\pi$  exchange as

$$\mathcal{M}_{DD}^{S\text{-wave corr. } 2\pi} = \frac{1}{\pi} \int_{4m_\pi^2}^{\infty} \frac{\rho_{00}^{(+)}(t')}{t-t'} dt', \quad \mathcal{M}_{DD}^{P\text{-wave corr. } 2\pi} = \frac{1}{\pi} \int_{4m_\pi^2}^{\infty} \frac{\rho_{11}^{(-)}(t')}{t-t'} dt', \quad (33)$$

as shown in Fig. 1. Here, we have suppressed the spin structure for the vector-isovector ( $\rho$ ) channel. Since  $D^*$  is a vector meson, the partial-wave expansions of the  $D^*\bar{D}^* \rightarrow \pi\pi$  and  $D^*\bar{D}^*$  are more involved because of the spin. Thus, we present the detailed calculation of deriving the spectral functions for the  $D^*\bar{D}^*$  amplitudes in Appendix A. The explicit expressions of the spectral functions for the  $D^*D^*$  channel are given as follows:

$$\begin{aligned} \rho_{00}^{(+),1}(t) &= \frac{3}{4M_{D^*}^2} \left[ \text{Im}p_1^{+,J=0}(t) - \text{Im}p_{1,\text{Born}}^{+,J=0}(t) \right], \\ \rho_{11}^{(-),1}(t) &= \frac{2}{(4M_{D^*}^2 - t)} \left[ \text{Im}p_1^{-,J=1}(t) - \text{Im}p_{1,\text{Born}}^{-,J=1}(t) \right], \\ \rho_{11}^{(-),2}(t) &= \frac{2M_{D^*}^2}{t(4M_{D^*}^2 - t)} \left[ \text{Im}p_2^{-,J=1}(t) - \text{Im}p_{2,\text{Born}}^{-,J=1}(t) \right], \\ \rho_{11}^{(-),3}(t) &= \frac{2M_{D^*}}{4\sqrt{t}(4M_{D^*}^2 - t)} \left[ \text{Im}p_3^{-,J=1}(t) - \text{Im}p_{3,\text{Born}}^{-,J=1}(t) \right], \end{aligned} \quad (34)$$

where the definitions of  $p_i^\pm$  can be found in Appendix A. The  $D^*D^*$  amplitudes with correlated  $2\pi$  exchange can be obtained by the dispersion relations, which are similar to Eq. (33).

### C. $\sigma$ and $\rho$ coupling constants

As shown in Eq. (33), we can determine the  $DD$  and  $D^*D^*$  amplitudes with correlated  $2\pi$  exchange. On the other hand, it is difficult to extract the  $\sigma$  and  $\rho$  coupling constants without any approximations. The best way to determine the coupling constants is first to compute the  $DD$  and  $D^*D^*$  amplitudes by using the effective Lagrangians, and then compare them to those with correlated  $2\pi$  exchange. Thus, we will first derive the  $DD$  and  $D^*D^*$  amplitudes based on the following effective Lagrangians:

$$\begin{aligned} \mathcal{L}_{DD\sigma} &= 2g_{DD\sigma}M_D DD^\dagger \sigma, \\ \mathcal{L}_{DD\rho} &= ig_{DD\rho} (D\boldsymbol{\tau} \cdot \boldsymbol{\rho}^\mu \partial_\mu D^\dagger - D^\dagger \boldsymbol{\tau} \cdot \boldsymbol{\rho}^\mu \partial_\mu D), \\ \mathcal{L}_{D^*D^*\sigma} &= 2M_{D^*}g_{D^*D^*\sigma}D^{*\mu}\bar{D}_\mu^*\sigma, \\ \mathcal{L}_{D^*D^*\rho} &= ig_{D^*D^*\rho}(\bar{D}^{*\nu}\boldsymbol{\tau} \cdot \boldsymbol{\rho}^\mu \partial_\mu D_\nu^* - D_\nu^*\boldsymbol{\tau} \cdot \boldsymbol{\rho}^\mu \partial_\mu \bar{D}_\nu^*) + 4if_{D^*D^*\rho}\bar{D}_\mu^*\boldsymbol{\tau} \cdot (\partial^\mu \boldsymbol{\rho}^\nu - \partial^\nu \boldsymbol{\rho}^\mu)D_\nu^*, \end{aligned} \quad (35)$$

where  $\sigma$  and  $\boldsymbol{\rho}_\mu$  denote the  $\sigma$ - and  $\rho$ -meson fields. We want to mention that for the  $DD\sigma$  and  $D^*D^*\sigma$  Lagrangians, we need to introduce additional dimensionful parameters, i.e., the masses of the  $D$  and  $D^*$  mesons, respectively. Here, the  $D$  and  $D^*$  mesons are not the scaled fields, which are different from  $P$  and  $P^*$  fields by the scaling factors  $(M_D)^{-1/2}$  and  $(M_{D^*})^{-1/2}$ , respectively. As for the  $D^*D^*\rho$  vertices, we have two different coupling constants, i.e., the vector coupling constant  $g_{D^*D^*\rho}$  and the tensor coupling constant  $f_{D^*D^*\rho}$ , which will be also determined in the present work.

Using the effective Lagrangians in Eq. (35), we obtain the invariant amplitudes for the  $DD \rightarrow DD$  and  $D^*D^* \rightarrow D^*D^*$  processes as follows:

$$\begin{aligned} \mathcal{M}_{DD}^\sigma(t) &= g_{DD\sigma}^2 \frac{4M_D^2}{t-m_\sigma^2}, \quad \mathcal{M}_{DD}^\rho(t, s) = g_{DD\rho}^2 \frac{s-u}{t-m_\rho^2}, \\ \mathcal{M}_{D^*D^*}^{\sigma, \lambda_1, \lambda_2, \lambda_3, \lambda_4}(t, s) &= 16\epsilon_\mu(\mathbf{p}, \lambda_1)\epsilon_\nu(-\mathbf{p}, \lambda_2)\epsilon_\alpha^*(\mathbf{p}', \lambda_3)\epsilon_\beta^*(-\mathbf{p}', \lambda_4) \frac{g_{D^*D^*\sigma}^2 M_{D^*}^2}{t-m_\sigma^2} \mathcal{A}^{\mu\nu\alpha\beta}, \\ \mathcal{M}_{D^*D^*}^{\rho, \lambda_1, \lambda_2, \lambda_3, \lambda_4}(t, s) &= \epsilon_\mu(\mathbf{p}, \lambda_1)\epsilon_\nu(-\mathbf{p}, \lambda_2) \left\{ 4g_{D^*D^*\rho}^2 \frac{s-u}{t-m_\rho^2} \mathcal{A}^{\mu\nu\alpha\beta} + 32\sqrt{3}f_{D^*D^*\rho}^2 \frac{t}{t-m_\rho^2} \mathcal{B}^{\mu\nu\alpha\beta} \right. \\ &\quad \left. + 16g_{D^*D^*\rho}f_{D^*D^*\rho} \frac{\sqrt{t(4M_{D^*}^2 - t)}}{t-m_\rho^2} \mathcal{C}^{\mu\nu\alpha\beta} \right\} \epsilon_\alpha^*(\mathbf{p}', \lambda_3)\epsilon_\beta^*(-\mathbf{p}', \lambda_4), \end{aligned} \quad (36)$$



where  $\lambda_i$  stand for the helicities of the corresponding  $D^*$  mesons in both the initial and final states.  $\mathcal{A}^{\mu\nu\alpha\beta}$ ,  $\mathcal{B}^{\mu\nu\alpha\beta}$  and  $\mathcal{C}^{\mu\nu\alpha\beta}$  denote the projection operators, which can be also found in Appendix A.

While the spectral functions we have explicitly derived in the present work as shown in Eqs. (32) and (34) contain information on the coupling strength for the  $\sigma$  and  $\rho$  mesons, it is rather difficult to extract the exact values of them. One possible way of extracting the coupling constants from the spectral functions is to make a pole approximation that is expressed, for example, by

$$\rho_{00}^{(+)}(t') = \pi g_{DD\sigma}^2 \delta(t' - m_\sigma^2), \quad \rho_{11}^{(-)}(t') = \pi g_{DD\rho}^2 \delta(t' - m_\rho^2), \quad (37)$$

where  $g_{DD\sigma}$  and  $g_{DD\rho}$  denote the *on-mass-shell* coupling constants for the  $DD\sigma$  and  $DD\rho$  vertices, respectively. These on-mass-shell coupling constants are used for the description of  $DD$  or  $DD\bar{D}$  reactions. Then we are able to reproduce all the amplitudes obtained from the effective Lagrangians such as

$$\frac{1}{\pi} \int_{4m_\pi^2}^{\infty} \frac{\rho_{00}^{(+)}(t')}{t - t'} dt' \approx \frac{g_{DD\sigma}^2}{t - m_\sigma^2}, \quad t \leq 0. \quad (38)$$

We can apply the same pole approximations to the  $D^*D^*$  case. Thus, the on-mass-shell coupling constants can be written by

$$\begin{aligned} g_{DD\sigma}^2 &\approx \frac{t - m_\sigma^2}{\pi} \int_{4m_\pi^2}^{\infty} \frac{\rho_{00}^{(+)}(t') dt'}{t - t'}, & g_{DD\rho}^2 &\approx \frac{t - m_\rho^2}{\pi} \int_{4m_\pi^2}^{\infty} \frac{\rho_{11}^{(-)}(t') dt'}{t - t'}, \\ g_{D^*D^*\sigma}^2 &\approx \frac{t - m_\sigma^2}{\pi} \int_{4m_\pi^2}^{\infty} \frac{\rho_{00}^{(+),1}(t') dt'}{t - t'}, & g_{D^*D^*\rho}^2 &\approx \frac{t - m_\rho^2}{\pi} \int_{4m_\pi^2}^{\infty} \frac{\rho_{11}^{(-),1}(t') dt'}{t - t'}, \\ f_{D^*D^*\rho}^2 &\approx \frac{t - m_\rho^2}{\pi} \int_{4m_\pi^2}^{\infty} \frac{\rho_{11}^{(-),2}(t') dt'}{t - t'}, & f_{D^*D^*\rho} g_{D^*D^*\rho} &\approx \frac{t - m_\rho^2}{\pi} \int_{4m_\pi^2}^{\infty} \frac{\rho_{11}^{(-),3}(t') dt'}{t - t'}, \end{aligned} \quad (39)$$

where  $t$  is the square of the momentum transfer in the  $s$  channel, i.e.,  $t \leq 0$ . Note that the left-hand sides of the above expressions contain the  $t$  variable. However, the approximated one-mass-shell coupling constants are almost independent of  $t$ . Only the numerical result of the  $D^*D^*\sigma$  coupling constant exhibits mild dependence on  $t$ , which comes from the broad width of the  $\sigma$  meson as implied in Eq. (39).

On the other hand, various works including lattice QCD [49–51] derive the coupling constants for the  $\rho$  meson not on the corresponding mass shell but at  $t = 0$ . Actually, the coupling constant at  $t = 0$  reflects the effect from a form factor that reduces the coupling strength by approximately a difference between the square of the cutoff mass and the mass of the corresponding exchanged meson. When exotic heavy mesons such as the  $X$ ,  $Y$ , and  $Z$  mesons are investigated in a meson-exchange picture, a monopole-type form factor is often used [29–32]. The transition amplitude for  $\sigma$  exchange is expressed as

$$\mathcal{T}_{DD}^\sigma(t) = \frac{g_{DD\sigma}^2}{t - m_\sigma^2} \left( \frac{\Lambda_\sigma^2 - m_\sigma^2}{\Lambda_\sigma^2 - t} \right)^2. \quad (40)$$

If we take into account Eq. (40) and the pole approximation given in Eq. (37), we are able to write a phenomenological expression for the vertex function  $g_{DD\sigma}(t)$

$$g_{DD\sigma}^2(t) = \frac{t - m_\sigma^2}{\pi} \int_{4m_\pi^2}^{\infty} \frac{\rho_{00}^{(+)}(t')}{t - t'} \left( \frac{\Lambda_\sigma^2 - t'}{\Lambda_\sigma^2 - t} \right)^2 dt', \quad t \leq 0, \quad (41)$$

where we have introduced a  $t'$ -dependent form factor

$$F(t, t') = \frac{\Lambda_\sigma^2 - t'}{\Lambda_\sigma^2 - t}. \quad (42)$$

A similar expression was used in the  $NN$  interaction [52]. The other vertex functions for the  $DD\rho$ ,  $D^*D^*\sigma$ , and  $D^*D^*\rho$  vertices can be written in a similar way. Using Eq. (41), we can compare the present results of the *off-mass-shell* coupling constants with those from other works at least phenomenologically.

Since the  $\sigma$  meson has a very broad mass, one has to examine the dependence of the coupling constants on the mass of the  $\sigma$  meson. Note that when we perform the integrals in Eq. (39) we take the upper limit to be  $52m_\pi^2$ , which was usually done in the case of the  $NN$  interaction. In fact, it is well known that the contributions from the spectral

functions at higher  $t'$  are rather small, when one considers the  $\sigma$  and  $\rho$  meson channels. As mentioned in Introduction, note that we have not included the  $K\bar{K}$  channel. In principle, we can introduce it, utilizing the coupled channel formalism. However, since we do not know the coupling constants for the  $D_s D^* K$ ,  $DD_s^* K$  and  $D^* D_s^* K$  vertices both experimentally and theoretically, we have to consider these coupling constants as free parameters, which brings about unavoidably additional uncertainties in the present work. Thus, we will take into account only the  $\pi\pi$  channel.

### III. RESULTS AND DISCUSSION

To compute first the off-shell  $D\bar{D} \rightarrow \pi\pi$  amplitudes in the pseudophysical region, we need to determine the coupling constants for the  $DD^*\pi$  and  $D^*D^*\pi$  vertices. we use the value of the  $g_{DD^*\pi}$  determined by the CLEO Collaboration [53, 54]. The  $g_{DD^*\pi}$  and  $g_{D^*D^*\pi}$  are related to the coupling  $g$  in the effective Lagrangians in Eq. (6) as follows:

$$g_{DD^*\pi} = \frac{2g}{f_\pi} \sqrt{M_D M_{D^*}}, \quad g_{D^*D^*\pi} = \frac{2g}{f_\pi}, \quad (43)$$

which can be found by using the decay rate of the  $D^*$  meson. The strong coupling  $g$  is known to be  $g = 0.59$ . We will use in this work the value determined by the CLEO Collaboration  $g_{DD^*\pi} = 17.9$ . If one considers the mass difference between the  $D$  and  $D^*$  mesons,  $g_{DD^*\pi}$  would become 17.3. As we have already discussed in the previous Section, we take the numerical values of the cutoff masses as  $\Lambda_{D^*} = 2.8$  GeV and  $\Lambda_D = 2.5$  GeV. The results depend marginally on the values of the cutoff masses. The uncertainty, which arises from the cutoff masses, is about 20 %. Then we can proceed to compute numerically the spectral functions for the  $DD$  and  $D^*D^*$  amplitudes with correlated  $2\pi$  exchange, which are expressed in Eqs. (32) and (34).

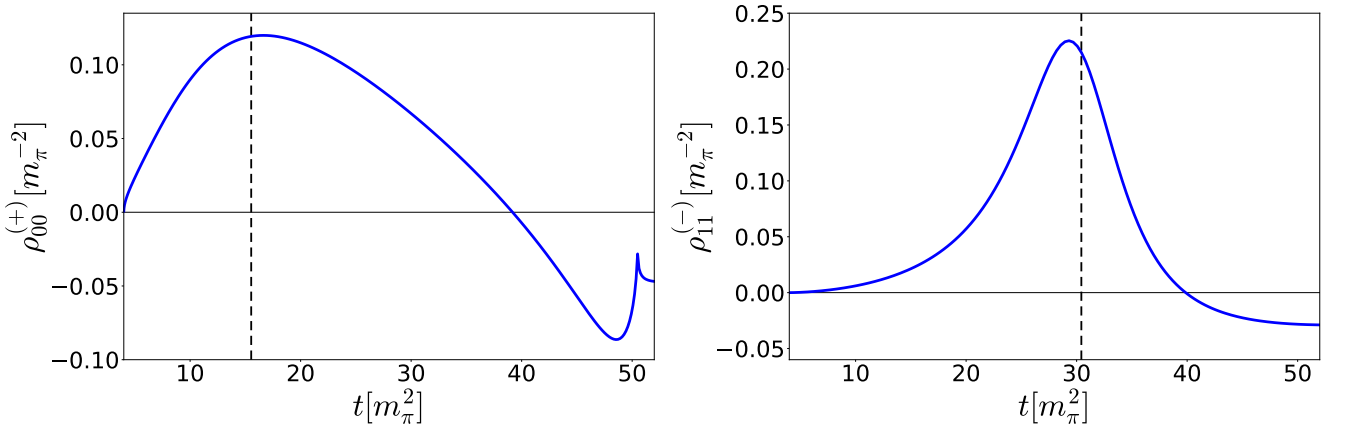


FIG. 5. The spectral function  $\rho_{00}^{(+)}$  (in the left panel) and  $\rho_{11}^{(-)}$  for the  $D\bar{D}$  channel as a function of  $t$  in unit of  $m_\pi^{-2}$ . Note that  $t$  denotes the square of the center-of-mass energy in the  $t$  channel. The dashed vertical line in the left panel corresponds to the  $\sigma$ -meson mass 550 MeV, whereas that in the right panel designates the  $\rho$ -meson mass 770 MeV.

In the left panel of Fig. 5, we draw the result of the spectral function  $\rho_{00}^{(+)}$ , of which the expression is given in Eq. (32). Its broad shape arises from the resonance of the  $\sigma$  meson with the large width. We see that the spectral function falls off after around  $t = 18m_\pi^2$  and then becomes negative from  $t = 30m_\pi^2$ , which is similar to the case of the  $N\bar{N}$  interaction [35]. Since the width of the  $\sigma$  meson is rather large, one should consider the dependence of the  $DD\sigma$  coupling constant on the mass of the  $\sigma$  meson,  $m_\sigma$ , which will be explicitly shown later. The right panel of Fig. 5 shows the result of  $\rho_{11}^{(-)}$  given in Eq. (32), which yields the  $g_{DD\rho}$  coupling constant. We observe that  $\rho_{11}^{(-)}$  becomes negative from around  $t = 40m_\pi^2$ , which is again similar to the  $N\bar{N}$  case in the  $\rho$  channel [35].

In the left panel of Fig. 6, we depict the result of the spectral function for the  $D^*\bar{D}^*$  case in the  $\sigma$  channel. It looks different from the corresponding  $D\bar{D}$  case. The reason is that the Born amplitudes for the  $D^*\bar{D}^* \rightarrow \pi\pi$  have rather strong dependence on  $t$ . Since we subtract the modulus squared of the Born amplitudes to avoid any double countings that arise from the whole  $2\pi$  exchange (see, for example, Eq. (32)), the  $D^*\bar{D}^*$  spectral function  $\rho_{00}^{(+),1}$  becomes negative already from around  $28m_\pi^2$ . In the right panel, we draw the result of  $\rho_{11}^{(-),1}$ , which is defined in Eq. (34). It will provide the vector coupling constant  $g_{D^*D^*\rho}$ . In the left and right panels of Fig. 7, we present the

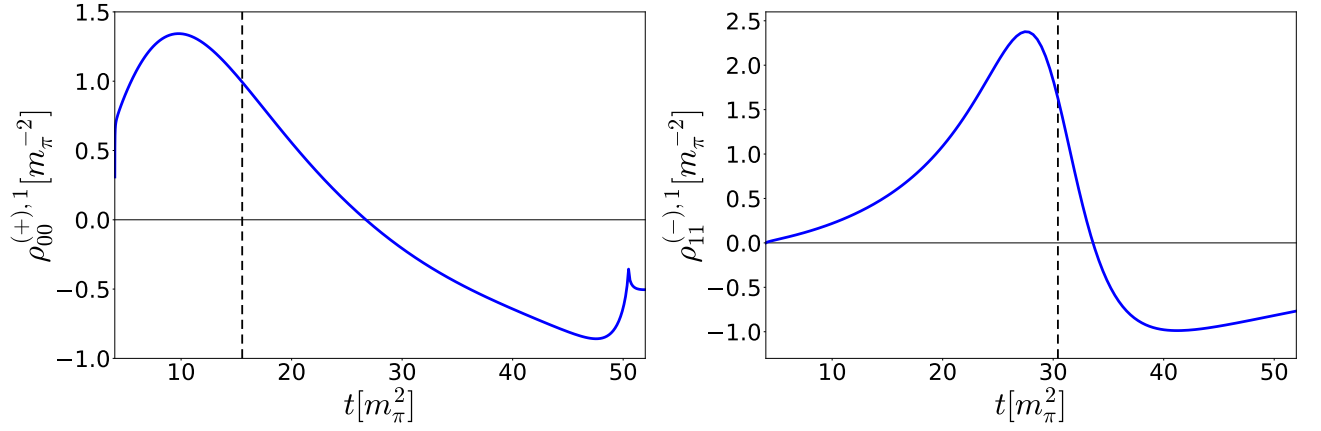


FIG. 6. The spectral function  $\rho_{00}^{(+),1}$  (left panel) and  $\rho_{11}^{(-),1}$  (right panel) for the  $D^*\bar{D}^*$  channel as a function of  $t$  in unit of  $m_\pi^{-2}$ . Notations are the same as in Fig. 5.

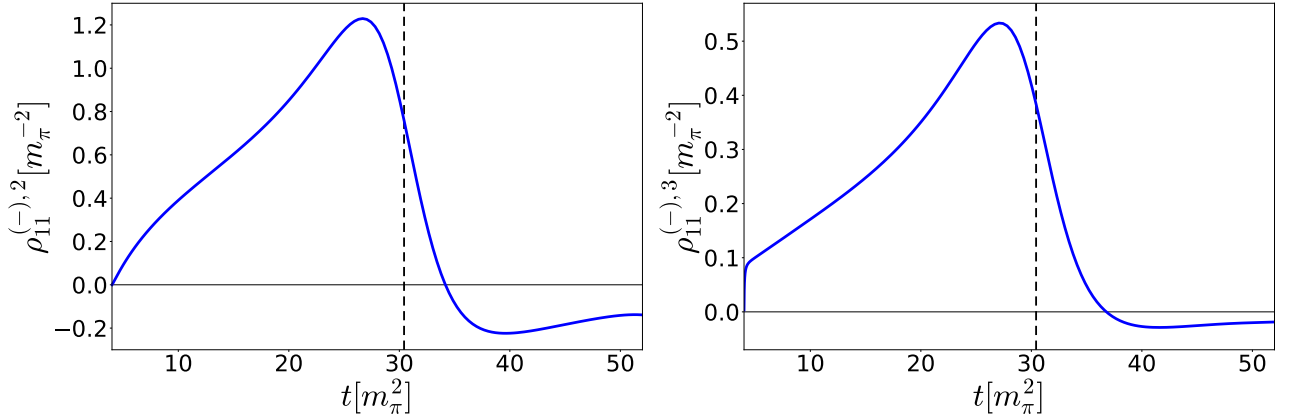


FIG. 7. The spectral functions  $\rho_{11}^{(-),2}$  (left panel) and  $\rho_{11}^{(-),3}$  (right panel) for the  $D^*\bar{D}^*$  channel as a function of  $t$  in unit of  $m_\pi^{-2}$ . Notations are the same as in Fig. 5.

numerical results of the spectral functions  $\rho_{11}^{(-),2}$  and  $\rho_{11}^{(-),3}$ , respectively. They are less affected by the subtraction of the Born terms, compared to the results of  $\rho_{11}^{(-),1}$ .

Before we extract the  $\sigma$  and  $\rho$  coupling constants, we first examine the transition amplitudes for  $DD \rightarrow DD$  and  $D^*D^* \rightarrow D^*D^*$  with  $S$ - and  $P$ -wave correlated  $2\pi$  exchange contributions, respectively. As we have mentioned already, the transition amplitudes for the  $DD$  and  $D^*D^*$  processes with  $\sigma$  and  $\rho$  exchanges given explicitly in Eq. (36) are compatible with those with  $S$ - and  $P$ -wave correlated  $2\pi$  exchanges, which are shown in Eq. (33). We use the values of the cutoff masses  $\Lambda_{\sigma(\rho)} = 1$  GeV, which is used in other works [29–32]. In Fig. 8 we draw the results for the  $DD$  and  $D^*D^*$  transition amplitudes with  $S$ - and  $P$ -wave correlated  $2\pi$  exchange contributions in Eq. (41). In the upper left panel, the present result for the  $DD$  amplitude with  $S$ -wave correlated  $2\pi$  exchange is depicted in the solid curve, compared with those with  $\sigma$  exchange as given in Eq. (40), for which the values of the  $DD\sigma$  coupling constant are taken from Refs. [29–31] and Ref. [32], respectively shown in the dashed and dotted curves.

The best way to determine the *on-mass-shell*  $\sigma$  and  $\rho$  coupling constants is to fit the  $DD$  and  $D^*D^*$  amplitudes presented in Fig. 8 by changing these coupling constants. Dot-dashed curves in Fig. 8 are extracted by fitting the  $\sigma$  and  $\rho$  coupling constants such that the  $\sigma$ - and  $\rho$ -exchange amplitudes reproduce the  $DD$  and  $D^*D^*$  amplitudes. As shown in the upper panels of Fig. 8, we are able to reproduce very well the  $DD$  amplitudes with  $S$ - and  $P$ -wave correlated  $2\pi$  exchanges. The  $DD\sigma$  and  $DD\rho$  coupling constants are determined to be  $g_{DD\sigma} = 1.50$  and  $g_{DD\rho} = 1.65$ , respectively. The present result lies between that with  $g_{DD\sigma} = 0.76$  [29–31] and that with  $g_{DD\sigma} = 3.4$  [32]. This implies that the extracted  $g_{DD\sigma}$  coupling constant from the present work should be found between these two values. On the other hand, the result for the  $DD$  amplitude with  $P$ -wave correlated  $2\pi$  exchange, which is drawn in the upper right panel of Fig. 8, is much weaker than those with the values of  $g_{DD\rho} = 3.71$  and  $2.6$ , taken respectively from Refs. [29–31] and Ref. [32].

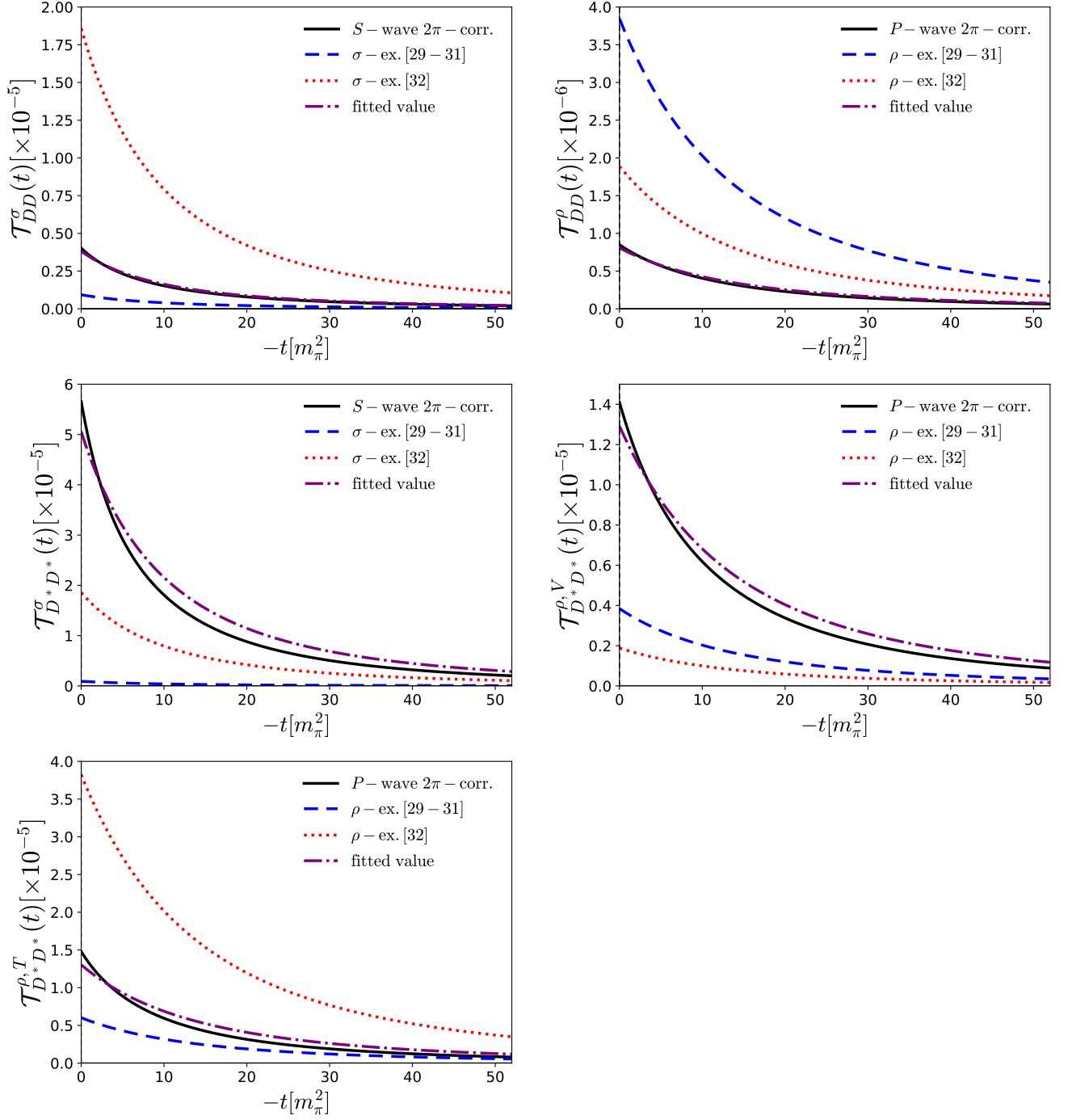


FIG. 8. The  $DD$  and  $D^*D^*$  amplitudes with  $S$ - and  $P$ -wave correlated  $2\pi$  exchange contributions, respectively. Solid curves depict the amplitudes with correlated  $2\pi$  exchange whereas dashed and dotted ones show the amplitudes produced by using the coupling constants taken from Refs. [29–31] and Ref. [32], respectively. Dash-dotted curves are obtained by fitting the  $\sigma$  and  $\rho$  coupling constants in such a way that the amplitudes with  $\sigma$  and  $\rho$  exchanges reproduce those with  $S$ - and  $P$ -wave correlated  $2\pi$  exchange, respectively.

The middle left panel of Fig. 8 shows that the present result for the  $D^*D^*$  amplitude with  $S$ -wave correlated  $2\pi$  exchange is greater than the other two results for those with  $g_{D^*D^*\sigma} = 0.76$  and  $3.4$ . The present results for the  $DD$  and  $D^*D^*$  amplitudes already indicate that  $g_{DD\sigma}$  and  $g_{D^*D^*\sigma}$  coupling constants are quite different. So far, many theoretical works on heavy meson interactions set these two  $\sigma$  coupling constants equal each other. However, if one considers correlated  $2\pi$  exchange, there is at least one reason why  $g_{DD\sigma}$  should be different from  $g_{D^*D^*\sigma}$ : While the  $D\bar{D} \rightarrow \pi\pi$  amplitude contains only  $D^*$  exchange, the  $D^*\bar{D}^* \rightarrow 2\pi$  amplitude has both  $D$  and  $D^*$  exchange. Thus,  $g_{D^*D^*\sigma}$  should be naturally greater than  $g_{DD\sigma}$  within the present framework. To determine the  $D^*D^*\sigma$  coupling constant, we again fit the  $D^*D^*$  amplitude with  $S$ -wave correlated  $2\pi$  exchange as done in the case of the  $DD\sigma$  coupling constant. The dot-dashed curve in the middle left panel of Fig. 8 depicts the numerical result for the  $D^*D^*$  amplitude with  $g_{D^*D^*\sigma} = 5.21$ , which describes well that with  $S$ -wave correlated  $2\pi$  exchange. This result indicates two important points: Firstly, the present result for the  $D^*D^*\sigma$  coupling constant is almost 3.5 times larger than that for  $g_{DD\sigma}$ . Secondly, the numerical value of  $g_{D^*D^*\sigma}$  is also much larger than those used in the other works [29–32].

In the middle right and lower left panels of Fig. 8 illustrate the present results for the  $D^*D^*$  amplitudes with vector and tensor  $P$ -wave correlated  $2\pi$  exchange, respectively. The comparisons of the present results to those with  $\rho$  meson exchange indicate that the vector  $D^*D^*\rho$  coupling constant extracted from this work should be larger than  $g_{D^*D^*\rho}$  of Refs. [29–32] whereas the value of the tensor coupling  $f_{D^*D^*\rho}$  from the present work should lie in between. Indeed, the numerical results for the vector and tensor  $D^*D^*\rho$  coupling constants are evaluated as follows:  $g_{D^*D^*\rho} = 6.47$  and  $f_{D^*D^*\rho} = 6.37$ . The results are summarized in Table I.

TABLE I.  $\sigma$  and  $\rho$  coupling constant for the  $D$  and  $D^*$  mesons. In the second column, the present results are listed. The third and fourth ones list the results from Refs. [29–31] and Ref. [32], respectively.

	Present work	[29–31]	[32]
$g_{DD\sigma}$	1.50	0.76	3.4
$g_{DD\rho}$	1.65	3.71	2.6
$g_{D^*D^*\sigma}$	5.21	0.76	3.4
$g_{D^*D^*\rho}$	6.47	3.71	2.6
$f_{D^*D^*\rho}$	6.37	4.64	11.7

We will now discuss the physical implications of the present results for the  $\sigma$  and  $\rho$  coupling constants in comparison with those used in the other works. Since there is no information on the  $DD\sigma$  coupling constant, the nonlinear sigma model has been often employed to determine  $g_{DD\sigma}$ . Furthermore, the coupling constant  $g_{D^*D^*\sigma}$  was naively set equal to  $g_{DD\sigma}$ , the heavy-quark spin symmetry being assumed. However, it is well known from the  $NN$  interaction that  $\sigma$  exchange arises from a pole approximation of  $S$ -wave (scalar-isoscalar) correlated  $2\pi$  exchange [33–35]. Moreover, the  $\sigma$  meson with broad width cannot be identified as the chiral partner of the pion. This implies that the  $\sigma$  coupling constant can only be quantitatively determined by considering the correlated  $2\pi$  exchange in the scalar-isoscalar channel. Note that the  $\sigma$  coupling constants for any hadrons are not just mere parameters but very dynamical ones. As shown in Table I and mentioned already previously, we find that the values of  $g_{D^*D^*\sigma}$  turn out different from those of  $g_{DD\sigma}$ . This can be understood by examining Fig. 3.  $D^*\bar{D}^* \rightarrow \pi\pi$  amplitudes receive contributions both from  $D$  and  $D^*$  exchange whereas the  $D\bar{D} \rightarrow \pi\pi$  amplitudes has only the contribution from  $D^*$  exchange, as we have already discussed previously. So, the magnitude of the  $D^*\bar{D}^* \rightarrow \pi\pi$  amplitudes is indeed larger than that of the  $D\bar{D} \rightarrow \pi\pi$  amplitudes. This indicates that  $g_{D^*D^*\sigma}$  should naturally be larger than  $g_{DD\sigma}$ . The present result is in contrast with those of Refs. [29–32] and Ref. [32]. Furthermore, there is no consensus on the values of both  $g_{DD\sigma}$  and  $g_{D^*D^*\sigma}$ . The present result for  $g_{DD\sigma}$  is approximately twice smaller than that of Ref. [32], whereas it is about two times larger than that used in Ref. [29–31]. On the other hand, it is other way around for the value of  $g_{D^*D^*\sigma}$ . The present result is approximately seven times larger than that of Ref. [29–31], while it is about 1.5 times larger than that of Ref. [32].

The  $DD\rho$  and  $D^*D^*\rho$  coupling constants are usually determined by using the vector-meson dominance [55]. Interestingly, Refs. [29–32] do not agree on the values of the  $\rho$ -meson couplings each other, even though they use the same vector-meson dominance. In particular, the values of the tensor coupling constant  $f_{D^*D^*\rho}$  differ by about 2.5 each other. This indicates that no clear consensus exists in the values for the  $\rho$ -meson coupling constants. They do come again yet from the  $P$ -wave correlated  $2\pi$  exchange in the vector-isovector channels. The present result for the  $DD\rho$  coupling constant is smaller than the results from Refs. [29–32]. The present value of the  $D^*D^*\rho$  vector coupling constant is quite larger than those of Refs. [29–32]. On the other hand, that of the tensor coupling constant  $f_{D^*D^*\rho}$  lies between that of Refs. [29–31] and that of Ref. [32]. In particular, it is approximately two times smaller than that of Ref. [32].

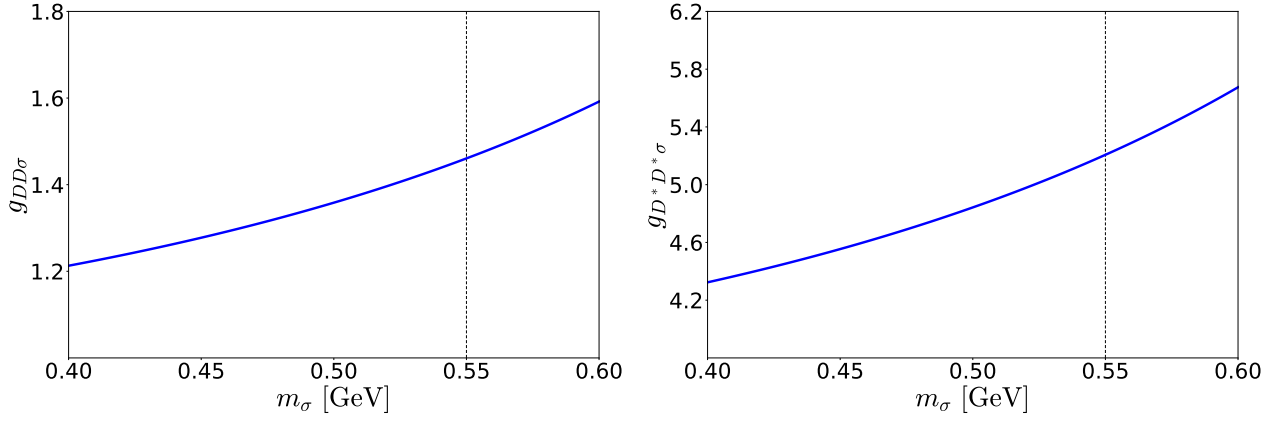


FIG. 9.  $DD\sigma$  and  $D^*D^*\sigma$  coupling constants as a function of the  $\sigma$ -meson mass.

Since the  $\sigma$ -meson has a broad mass distribution, it is rather difficult to determine its precise mass. Thus, it is of great importance to see if the  $\sigma$  coupling constants are sensitive to the value of  $m_\sigma$ . The left and right panels of Fig. 9 draw the dependence of  $g_{DD\sigma}$  and  $g_{D^*D^*\sigma}$  on the  $\sigma$ -meson mass, respectively. The dashed vertical line represents a preferable value for the  $\sigma$ -meson mass, i.e.  $m_\sigma = 0.55$  GeV, which was often taken in the  $NN$  interactions. The values of  $g_{DD\sigma}$  and  $g_{D^*D^*\sigma}$  increase mildly as  $m_\sigma$  increases. We will take the  $\sigma$  coupling constants at  $m_\sigma = 550$  MeV as our final results.

As mentioned previously, the values of the coupling constants from lattice QCD and other works are often derived at  $t = 0$ , which are off mass-shell. In the present work, we can only obtain the *on-mass-shell* coupling constants. In order to extend the present results to the off-mass-shell region,  $t \leq 0$ , we need to utilize phenomenologically monopole-type form factors, which are often employed by various works in studying properties of the exotic heavy mesons in meson-exchange pictures. Thus, we introduce a form factor given in Eq. (41), which is reduced to the usual monopole-type form factor with the pole approximation. Though Eq. (41) is a phenomenological one, it is still very useful for the comparison of the present results with those from other works at  $t = 0$ . In Fig. 10, we depict the numerical results for the vertex functions of the  $\sigma$  and  $\rho$  mesons both in the  $DD$  and  $D^*D^*$  channels as functions of the squared momentum transfer  $-t$ , comparing them obtained by using the  $\sigma$  and  $\rho$  coupling constants taken from Refs. [29–32]. In the first panel of Fig. 10, we draw the present result for  $g_{DD\sigma}(t)$  in the solid curve, while the dashed and dotted ones correspond to Refs. [29–31] and Ref. [32], respectively. The dot-dashed curves illustrate the vertex functions with the present values of  $\sigma$  and  $\rho$  coupling constants. Note that the *off-mass-shell* coupling constants are reduced by approximately 30 %. This can be easily understood by the following value of the monopole-type form factor

$$\frac{\Lambda_\sigma^2 - m_\sigma^2}{\Lambda_\sigma^2} \approx 0.7. \quad (44)$$

We have similar conclusions also on the  $DD\rho$  and  $D^*D^*\rho$  coupling constants. However, since the mass of the  $\rho$  meson is about 770 MeV, the  $\rho$  coupling constants are reduced by about 60 %. Thus, we summarize the present results for the *off-mass-shell*  $\sigma$  and  $\rho$  coupling constants at  $t = 0$  as follows:

$$g_{DD\sigma}(0) = 1.07, \quad g_{D^*D^*\sigma}(0) = 3.91, \quad (45)$$

$$g_{DD\rho}(0) = 0.69, \quad g_{D^*D^*\rho}(0) = 2.77, \quad f_{D^*D^*\rho}(0) = 2.78. \quad (46)$$

The results for the  $g_{DD\rho}$  and  $g_{D^*D^*\rho}$  from lattice QCD [49] at  $t = 0$  are given as

$$g_{DD\rho}(0) = 4.84(34), \quad g_{D^*D^*\rho}(0) = 5.94(56), \quad \text{lattice QCD [49]}. \quad (47)$$

Comparing the present values with those from other works, we find that the present results are underestimated. The results from Refs. [50, 51] are larger than the present value for the  $DD\rho$  coupling constant:

$$\begin{aligned} g_{DD\rho}(0) &= 2.9, \quad \text{QCD sum rule [50]}, \\ g_{DD\rho}(0) &= 6.37, \quad \text{Dyson-Schwinger approach [51]}. \end{aligned} \quad (48)$$

It is straightforward to compute the  $\sigma$  and  $\rho$  coupling constants for the  $B$  and  $B^*$  mesons because of the heavy quark flavor symmetry. However, there are still subtle points that arise from the mass difference between the charm

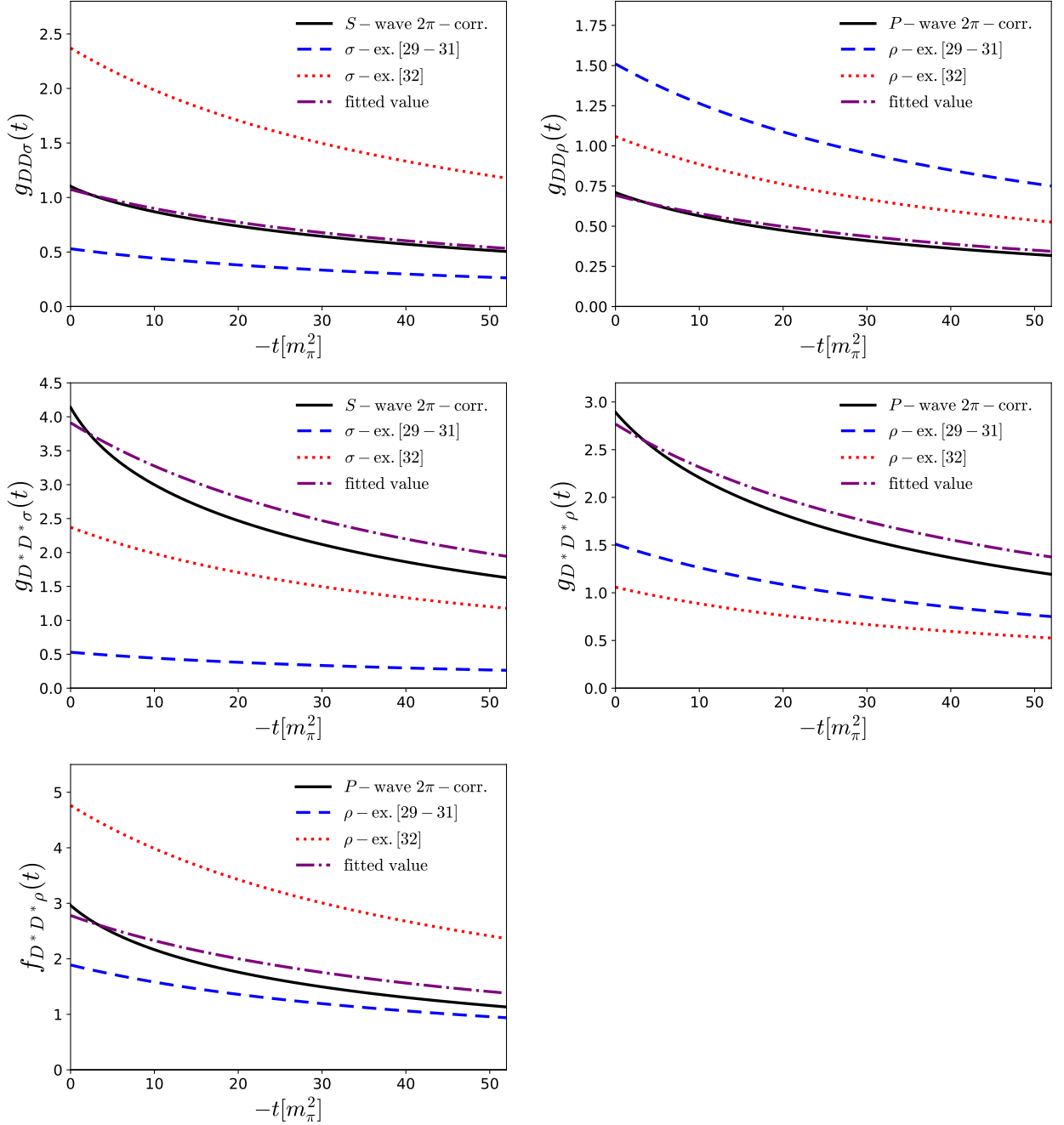


FIG. 10. Numerical results for the  $\sigma$  and  $\rho$  vertex functions with correlated  $2\pi$  exchange in comparison with those with monopole-type form factors. The solid curves draw the present results defined in Eq. (41) whereas dashed and dotted ones show the  $t$  dependence of the vertex functions produced by using the coupling constants given in Refs. [29–31] and Ref. [32], respectively. The dot-dashed curves illustrate the fitted coupling constant by using the monopole-type form factor.

and beauty quarks. Since the  $B$  and  $B^*$  mesons are much heavier than the  $D$  and  $D^*$  mesons, we need to introduce larger values of the cutoff masses, i.e.  $\Lambda = 6.1$  GeV, which is about 800 MeV larger than the  $B$  meson mass. The amplitudes remain almost stable when the cut-off mass is changed. Another input for the results given in Table II is the  $BB^*\pi$  coupling constant, of which the value is  $g_{BB^*\pi} = \frac{2g}{f_\pi} \sqrt{M_B M_{B^*}} = 45$ . Compared with that of  $g_{DD^*\pi} = 17.9$ ,  $g_{BB^*\pi}$  is approximately 2.5 times larger. Due to the heavy quark flavor symmetry,  $g_{B^*B^*\pi}$  has the same expression as that of  $g_{D^*D^*\pi}$ .

In Table II we list the results on the  $\sigma$  and  $\rho$  coupling constants for the  $B$  and  $B^*$  mesons. We observe that magnitudes of the coupling constants for the  $B$  and  $B^*$  mesons are much larger than those of  $D$  and  $D^*$  mesons in

TABLE II.  $\sigma$  and  $\rho$  coupling constant for the  $B$  and  $B^*$  mesons. In the second column, the present results are listed. The third and fourth ones list the results from Refs. [29–31] and Ref. [32], respectively.

	Present work	[29–31]	[32]
$g_{BB\sigma}$	7.05	0.76	3.4
$g_{BB\rho}$	8.92	3.71	2.6
$g_{B^*B^*\sigma}$	9.47	0.76	3.4
$g_{B^*B^*\rho}$	10.1	3.71	2.6
$f_{B^*B^*\rho}$	29.8	4.64	11.7

Table I. This can be easily understood from the fact that the value of the  $BB^*\pi$  coupling constant is much larger than that of  $DD^*\pi$ . Thus, it is very unlikely that the  $\sigma$  and  $\rho$  coupling constants for the  $B$  and  $B^*$  mesons are set to be the same as those for the  $D$  and  $D^*$  based on the heavy quark symmetry. In fact, Refs. [29–32] put them equal to those for the  $D$  and  $D^*$  mesons. However, the present results show that these coupling constants are much larger than those for the  $D$  and  $D^*$  mesons as shown in Table II. Even though theoretical uncertainties of the present work are considered, we can draw a clear conclusion that the  $\sigma$  and  $\rho$  coupling constants for  $B$  and  $B^*$  mesons should be taken to be at least larger than those for the  $D$  and  $D^*$  mesons. It indicates that these large values of the coupling constants may come into significant role in describing the molecular states consisting of  $B\bar{B}$  and  $B\bar{B}^*$ .

#### IV. SUMMARY AND CONCLUSION

In the present work, we derived the five coupling constants, i.e., the  $DD\sigma$ ,  $DD\rho$ ,  $D^*D^*\sigma$ , vector and tensor  $D^*D^*\rho$  coupling constants, having constructed the spectral functions in both the scalar-isoscalar ( $\sigma$ ) and vector-isovector ( $\rho$ ) channels. Starting from the effective Lagrangians, we first computed the off-shell  $D\bar{D} \rightarrow \pi\pi$  and  $D^*\bar{D}^* \rightarrow \pi\pi$  amplitudes in the pseudophysical region that is defined in the range of  $4m_\pi^2 \leq t \leq 52m_\pi^2$ . Then we combined these off-shell Born amplitudes with the off-shell  $\pi\pi$  amplitudes that was evaluated within the framework of the meson-exchange model known as the Jülich  $\pi\pi$  model, making use of the Blankenbecler-Sugar rescattering equation. Imposing the two-body unitarity, we were able to evaluate the spectral functions of correlated  $2\pi$  exchange for the  $D\bar{D}$  and  $D^*\bar{D}^*$  interactions. The  $DD$  and  $D^*D^*$  amplitudes with correlated  $2\pi$  exchange were derived by the dispersion relations. We presented the  $DD$  and  $D^*D^*$  amplitudes with  $S$ - and  $P$ -wave correlated  $2\pi$  exchange, comparing them with the corresponding ones with  $\sigma$  and  $\rho$  meson exchanges, respectively. By reproducing the  $DD$  and  $D^*D^*$  amplitudes with  $S$ - and  $P$ -wave correlated  $2\pi$  exchange, we obtained the numerical results on the *on-mass-shell* coupling constants and compared them with those of other works. Having introduced a monopole-like form factor, we discussed the coupling constants in the region  $t \leq 0$ . Compared with the lattice data, the present results are quite smaller than them. We also examined the dependence of the  $\sigma$  couplings on the  $\sigma$ -meson mass. We computed the  $\sigma$  and  $\rho$  coupling constants for the  $B$  and  $B^*$  mesons for completeness. We found that these coupling constants for the beauty mesons are much larger than those for the  $D$  and  $D^*$  mesons. The reason comes from the fact that the  $BB^*\pi$  coupling constants are much greater than  $DD^*\pi$  ones. It leads to the conclusion that it is unlikely for the  $\sigma$  and  $\rho$  coupling constants for the  $B$  and  $B^*$  mesons to be the same as those for the charmed mesons.

The present results can be used in any one-boson exchange model for the description of the exotic heavy mesons as weakly bound molecular states such as the  $X(3872)$  exotic mesons. Though the two-boson exchange may be considered to be small, the effects of the correlated  $2\pi$  exchange may play a very important role in understanding those exotic mesons. In particular, considering the fact that the  $\sigma$ -meson exchange is the main source for the attraction between heavy mesons such as  $D$  and  $D^*$  as in the case of the  $NN$  interactions, the present determination of the  $\sigma$  couplings for heavy mesons will be rather useful for understanding the exotic heavy mesons. We can also determine the  $\sigma$  and  $\rho$  couplings for the other processes such as the  $D_1\bar{D}^*$  and  $D_s\bar{D}^*$  interactions. The corresponding works are under way.

#### ACKNOWLEDGMENTS

The present work is supported by Inha University Research Grant in 2019 (No. 61489-01).



### Appendix A: The derivation of the spetral functions for the $D^*D^*$ channel

The projection operators for the vector and tensor coupling constants in the  $s$  channel are defined as

$$\begin{aligned}\mathcal{A}^{\mu\nu\alpha\beta} &= \frac{1}{4}g^{\mu\alpha}g^{\nu\beta}, \\ \mathcal{B}^{\mu\nu\alpha\beta} &= \frac{1}{2\sqrt{3}t}(g^{\alpha\nu}k^\mu k^\beta - g^{\alpha\beta}k^\mu k^\nu - g^{\mu\nu}k^\alpha k^\beta + g^{\beta\mu}k^\alpha k^\nu), \\ \mathcal{C}^{\mu\nu\alpha\beta} &= \frac{1}{4\sqrt{t(4M_{D^*}^2 - t)}}(-g^{\nu\beta}k^\mu P_2^\alpha + g^{\nu\beta}P_2^\mu k^\alpha - g^{\mu\alpha}P_1^\nu k^\beta + g^{\mu\alpha}k^\nu P_1^\beta),\end{aligned}\tag{A1}$$

where

$$k = p_1 - p_3 = p_4 - p_2, \quad P_1 = p_1 + p_3, \quad P_2 = p_2 + p_4.\tag{A2}$$

In the  $t$  channel, they can be reexpressed as

$$\begin{aligned}\bar{\mathcal{A}}^{\mu\nu\alpha\beta} &= \frac{1}{4}g^{\mu\alpha}g^{\nu\beta}, \\ \bar{\mathcal{B}}^{\mu\nu\alpha\beta} &= \frac{1}{2\sqrt{3}t}(g^{\alpha\nu}P^\mu P^\beta - g^{\alpha\beta}P^\mu P^\nu - g^{\mu\nu}P^\alpha P^\beta + g^{\beta\mu}P^\alpha P^\nu), \\ \bar{\mathcal{C}}^{\mu\nu\alpha\beta} &= \frac{1}{4\sqrt{t(4M_{D^*}^2 - t)}}(-g^{\nu\beta}P^\mu \bar{P}_2^\alpha + g^{\nu\beta}\bar{P}_2^\mu P^\alpha - g^{\mu\alpha}\bar{P}_1^\nu P^\beta + g^{\mu\alpha}P^\nu \bar{P}_1^\beta),\end{aligned}\tag{A3}$$

where

$$P = p_1 + \bar{p}_3 = \bar{p}_2 + p_4, \quad \bar{P}_1 = p_1 - \bar{p}_3, \quad \bar{P}_2 = p_4 - \bar{p}_2.\tag{A4}$$

The imaginary parts of the  $D^*\bar{D}^*$  amplitudes are written as

$$\begin{aligned}\text{Im } \mathcal{M}_{D^*D^*\sigma} &= 16M_{D^*}^2 \epsilon_\mu(\mathbf{p}, \lambda_1) \epsilon_\alpha(-\mathbf{p}, \lambda_3) \epsilon_\nu^*(-\mathbf{p}', \lambda_2) \epsilon_\beta^*(\mathbf{p}', \lambda_4) \bar{\mathcal{A}}^{\mu\nu\alpha\beta} \rho_{00}^{(+),1}(t), \\ &= \text{Im } p_1^{+,J=0}(t)\end{aligned}\tag{A5}$$

and

$$\begin{aligned}\text{Im } \mathcal{M}_{D^*\bar{D}^*\rho} &= \epsilon_\mu(\mathbf{p}, \lambda_1) \epsilon_\alpha(-\mathbf{p}, \lambda_3) \left[ \rho_{11}^{(-),1}(t) 4(s-u) \bar{\mathcal{A}}^{\mu\nu\alpha\beta} \right. \\ &\quad \left. + \rho_{11}^{(-),2}(t) 32\sqrt{3}t \bar{\mathcal{B}}^{\mu\nu\alpha\beta} + \rho_{11}^{(-),3}(t) 16\sqrt{t(4M_{D^*}^2 - t)} \bar{\mathcal{C}}^{\mu\nu\alpha\beta} \right] \epsilon_\nu^*(-\mathbf{p}', \lambda_2) \epsilon_\beta^*(\mathbf{p}', \lambda_4), \\ &= 2 \text{Im } p_1^{-,J=1}(t) d_{00}^1(\cos\theta) + 2 \text{Im } p_2^{-,J=1}(t) d_{1,-1}^1(\cos\theta) + 2 \text{Im } p_3^{-,J=1}(t) d_{0,1}^1(\cos\theta).\end{aligned}\tag{A6}$$

The  $p_i^{\pm,J}$  are defined as

$$\begin{aligned}\text{Im } p_1^{+,J=0} &\equiv \frac{1}{64\pi} \sqrt{\frac{t-4m_\pi^2}{t}} |\mathcal{M}_{D^*\bar{D}^*\rightarrow\pi\pi}^{(+),J=0}(1,1)|^2, \\ \text{Im } p_1^{-,J=1} &\equiv \frac{1}{64\pi} \sqrt{\frac{t-4m_\pi^2}{t}} |\mathcal{M}_{D^*\bar{D}^*\rightarrow\pi\pi}^{(-),J=1}(1,1)|^2, \\ \text{Im } p_2^{-,J=1} &\equiv \frac{1}{64\pi} \sqrt{\frac{t-4m_\pi^2}{t}} |\mathcal{M}_{D^*\bar{D}^*\rightarrow\pi\pi}^{(-),J=1}(1,0)|^2, \\ \text{Im } p_3^{-,J=1} &\equiv \frac{1}{64\pi} \sqrt{\frac{t-4m_\pi^2}{t}} \text{Re} \left\{ \mathcal{M}_{D^*\bar{D}^*\rightarrow\pi\pi}^{(-),J=1\dagger}(0,1) \mathcal{M}_{D^*\bar{D}^*\rightarrow\pi\pi}^{(-),J=1}(1,1) \right\}.\end{aligned}\tag{A7}$$

After subtraction of the Born amplitudes, we find the spectral functions as follows:

$$\begin{aligned}
\rho_{00}^{(+),1}(t) &= \frac{3}{4M_{D^*}^2} \left[ \text{Im } p_1^{+,J=0}(t) - \text{Im } p_{1,\text{Born}}^{+,J=0}(t) \right], \\
\rho_{11}^{(-),1}(t) &= \frac{2}{4M_{D^*}^2 - t} \left[ \text{Im } p_1^{-,J=1}(t) - \text{Im } p_{1,\text{Born}}^{-,J=1}(t) \right], \\
\rho_{11}^{(-),2}(t) &= \frac{2M_{D^*}^2}{t(4M_{D^*}^2 - t)} \left[ \text{Im } p_2^{-,J=1}(t) - \text{Im } p_{2,\text{Born}}^{-,J=1}(t) \right], \\
\rho_{11}^{(-),3}(t) &= \frac{2M_{D^*}}{4\sqrt{t}(4M_{D^*}^2 - t)} \left[ \text{Im } p_3^{-,J=1}(t) - \text{Im } p_{3,\text{Born}}^{-,J=1}(t) \right].
\end{aligned} \tag{A8}$$

- 
- [1] E. S. Swanson, Phys. Rept. **429** (2006) 243 [hep-ph/0601110].
  - [2] H. X. Chen, W. Chen, X. Liu and S. L. Zhu, Phys. Rept. **639** (2016) 1 [arXiv:1601.02092 [hep-ph]].
  - [3] R. F. Lebed, R. E. Mitchell and E. S. Swanson, Prog. Part. Nucl. Phys. **93** (2017) 143 [arXiv:1610.04528 [hep-ph]].
  - [4] S. L. Olsen, T. Skwarnicki and D. Zieminska, Rev. Mod. Phys. **90** (2018) 015003 [arXiv:1708.04012 [hep-ph]].
  - [5] F. K. Guo, C. Hanhart, U. G. Meissner, Q. Wang, Q. Zhao and B. S. Zou, Rev. Mod. Phys. **90** (2018) 015004 [arXiv:1705.00141 [hep-ph]].
  - [6] S. K. Choi *et al.* [Belle Collaboration], Phys. Rev. Lett. **91** (2003) 262001 [hep-ex/0309032].
  - [7] D. Acosta *et al.* [CDF Collaboration], Phys. Rev. Lett. **93** (2004) 072001 [hep-ex/0312021].
  - [8] V. M. Abazov *et al.* [D0 Collaboration], Phys. Rev. Lett. **93** (2004) 162002 [hep-ex/0405004].
  - [9] R. Aaij *et al.* [LHCb Collaboration], Eur. Phys. J. C **72** (2012) 1972 [arXiv:1112.5310 [hep-ex]].
  - [10] V. Chiochia [CMS Collaboration], EPJ Web Conf. **28** (2012) 4011 [arXiv:1201.6677 [hep-ex]].
  - [11] E. Eichten and F. Feinberg, Phys. Rev. D **23** (1981) 2724.
  - [12] S. Godfrey and N. Isgur, Phys. Rev. D **32** (1985) 189.
  - [13] S. N. Gupta, S. F. Radford and W. W. Repko, Phys. Rev. D **34** (1986) 201.
  - [14] L. P. Fulcher, Phys. Rev. D **44** (1991) 2079.
  - [15] J. Zeng, J. W. Van Orden and W. Roberts, Phys. Rev. D **52** (1995) 5229 [hep-ph/9412269].
  - [16] D. Ebert, R. N. Faustov and V. O. Galkin, Phys. Rev. D **67** (2003) 014027 [hep-ph/0210381].
  - [17] E. J. Eichten, K. Lane and C. Quigg, Phys. Rev. Lett. **89** (2002) 162002 [hep-ph/0206018].
  - [18] S. Pakvasa and M. Suzuki, Phys. Lett. B **579** (2004) 67 [hep-ph/0309294].
  - [19] L. Maiani, F. Piccinini, A. D. Polosa and V. Riquer, Phys. Rev. D **71** (2005) 014028 [hep-ph/0412098].
  - [20] H. Hogaasen, J. M. Richard and P. Sorba, Phys. Rev. D **73** (2006) 054013 [hep-ph/0511039].
  - [21] D. Ebert, R. N. Faustov and V. O. Galkin, Phys. Lett. B **634** (2006) 214 [hep-ph/0512230].
  - [22] B. A. Li, Phys. Lett. B **605** (2005) 306 [hep-ph/0410264].
  - [23] N. A. Tornqvist, Z. Phys. C **61** (1994) 525 [hep-ph/9310247].
  - [24] N. A. Törnqvist, hep-ph/0308277.
  - [25] F. E. Close and P. R. Page, Phys. Lett. B **578** (2004) 119 [hep-ph/0309253].
  - [26] M. B. Voloshin, Phys. Lett. B **579** (2004) 316 [hep-ph/0309307].
  - [27] C. -Y. Wong, Phys. Rev. C **69** (2004) 055202 [hep-ph/0311088].
  - [28] R. Aaij *et al.* [LHCb Collaboration], Phys. Rev. D **92** (2015) no.1, 011102 [arXiv:1504.06339 [hep-ex]].
  - [29] X. Liu, Z. G. Luo, Y. R. Liu and S. L. Zhu, Eur. Phys. J. C **61** (2009) 411 [arXiv:0808.0073 [hep-ph]].
  - [30] I. W. Lee, A. Faessler, T. Gutsche and V. E. Lyubovitskij, Phys. Rev. D **80** (2009) 094005 [arXiv:0910.1009 [hep-ph]].
  - [31] Y. R. Liu, M. Oka, M. Takizawa, X. Liu, W. Z. Deng and S. L. Zhu, Phys. Rev. D **82** (2010) 014011 [arXiv:1005.2262 [hep-ph]].
  - [32] M. Z. Liu, T. W. Wu, M. Pavon Valderrama, J. J. Xie and L. S. Geng, Phys. Rev. D **99** (2019) 094018 [arXiv:1902.03044 [hep-ph]].
  - [33] G. E. Brown and A. D. Jackson, “*The Nucleon-Nucleon Interaction*”, (North-Holland Pub., New York, 1976).
  - [34] R. Machleidt, K. Holinde and C. Elster, Phys. Rept. **149** (1987) 1.
  - [35] H. -Ch. Kim, J. W. Durso and K. Holinde, Phys. Rev. C **49** (1994) 2355.
  - [36] H.-Ch. Kim and M. Shmatikov, Phys. Lett. B **375**, 310 (1996) [hep-ph/9506372].
  - [37] J. W. Durso, A. D. Jackson and B. J. Verwest, Nucl. Phys. A **345** (1980) 471.
  - [38] A. Reuber, K. Holinde, H. C. Kim and J. Speth, Nucl. Phys. A **608**, 243 (1996) [nucl-th/9511011].
  - [39] D. Lohse, J. W. Durso, K. Holinde and J. Speth, Nucl. Phys. A **516** (1990) 513.
  - [40] G. Janssen, B. C. Pearce, K. Holinde and J. Speth, Phys. Rev. D **52** (1995) 2690 [nucl-th/9411021].
  - [41] M. B. Wise, Phys. Rev. D **45** (1992) R2188.
  - [42] T. M. Yan, H. Y. Cheng, C. Y. Cheung, G. L. Lin, Y. C. Lin and H. L. Yu, Phys. Rev. D **46** (1992) 1148 Erratum: [Phys. Rev. D **55** (1997) 5851].
  - [43] M. B. Wise, In “Beijing 1993, Proceedings, Particle physics at the Fermi scale\* 71-114, and Caltech Pasadena - CALT-68-1860 (93,rec.Jul.) 48 p [hep-ph/9306277].

- [44] G. Burdman and J. F. Donoghue, Phys. Lett. B **280** (1992) 287.
- [45] C. G. Callan, Jr., S. R. Coleman, J. Wess and B. Zumino, Phys. Rev. **177** (1969) 2247.
- [46] W. R. Frazer and J. R. Fulco, Phys. Rev. **117** (1960) 1603.
- [47] J. Y. Kim and H.-Ch. Kim, Phys. Rev. D **97** (2018) 114009 [arXiv:1803.04069 [hep-ph]].
- [48] R. Blankenbecler and R. Sugar, Phys. Rev. **142** (1966) 1051.
- [49] K. Can, G. Erkol, M. Oka, A. Ozpineci and T. Takahashi, Phys. Lett. B **719** (2013) 103 [arXiv:1210.0869 [hep-lat]].
- [50] M. Bracco, M. Chiapparini, A. Lozea, F. Navarra and M. Nielsen, Phys. Lett. B **521** (2001) 1 [arXiv:hep-ph/0108223 [hep-ph]].
- [51] B. El-Bennich, M. A. Paracha, C. D. Roberts and E. Rojas, Phys. Rev. D **95** (2017) 034037 [arXiv:1604.01861 [nucl-th]].
- [52] H.-Ch. Kim, “*A Microscopic model for correlated 2 pi exchange in free nucleon-nucleon scattering and in nuclear matter*,” Dissertation, Jülich KFA - Jül-2771, (1993).
- [53] S. Ahmed *et al.* [CLEO Collaboration], Phys. Rev. Lett. **87** (2001) 251801 [hep-ex/0108013].
- [54] A. Anastassov *et al.* [CLEO Collaboration], Phys. Rev. D **65** (2002) 032003 [hep-ex/0108043].
- [55] R. Casalbuoni, A. Deandrea, N. Di Bartolomeo, R. Gatto, F. Feruglio and G. Nardulli, Phys. Lett. B **299** (1993) 139 [hep-ph/9211248].